# CHAPTER TWO

# Tissue anti-adhesion potential of selected polyhydroxybutyrate biomaterials in a rat model

# 1. Introduction

Adhesions resulting from surgical procedures can cause considerable pain, bowel obstruction and impair fertility in women. The incidence of intraperitoneal adhesions ranges from 67 to 93% after general surgical abdominal operations and up to 97% following open gynecological pelvic procedures [128]. Adhesions form between the wound and the omentum in over 80% of patients and these adhesions may involve the intestines in 50% of patients [128]. One of the most serious consequences of peritoneal adhesion is small bowel obstruction. Within 2 years of surgery, 14% of patients may develop adhesive intestinal obstruction [297]. Indeed, postoperative adhesions have a profound economic and health impacts, including the surgical procedure itself, hospitalization, recuperation, lost productivity and poor health-related quality of life [298]. It has been estimated that in the United States, there are 117 hospitalizations for adhesion-related problems per 100 000 people, and the total cost for hospital and surgical expenditure is about $1.3 billion [298]. In some European countries, the direct medical costs for adhesion-related problems are more than the surgical expenditure for gastric cancer and almost as much as those for rectal cancer [299]. Thus, effective strategies for adhesion prevention will help to reduce tissue adhesion management costs and unnecessary morbidity and mortality rates.

Tissue adhesion is a natural consequence of surgery when the damaged tissue begins to heal as inflammation of the peritoneum results into fibrinous exudates that organize into adhesion bands [131]. Adhesion formation is associated with significant oxidative stress, both from the activation of the mesothelium and underlying endothelial cells and, more importantly, from the infiltration and subsequent activation of neutrophils, macrophages and cytokines [268]. Aside from normal peritoneal regeneration, the process of postoperative peritoneal adhesion may be considered as the pathological part of healing following any peritoneal injury [300]. Peritoneal injury, due to surgery, infection or irritation, initiates inflammation with fibrinous exudate and fibrin formation. The balance between fibrin deposition and degradation is crucial in determining normal peritoneal healing or adhesion formation. If fibrin is completely degraded, normal peritoneal healing may occur. In contrast, incompletely degraded fibrin results in peritoneal adhesions [301].

Activation of the fibrinolytic system results in the conversion of plasminogen into plasmin which is highly effective in the degradation of fibrin into fibrin degradation products. Tissue-type plasminogen activator (tPA) and urokinase-type plasminogen (uPA) activate plasminogen [302]. Following surgery, the equilibrium between coagulation and fibrinolysis is disturbed, in favor of the coagulation system. Plasminogen activation is hampered by plasminogen-activating inhibitors (PAI)-1, 2 and 3 through formation of inactive complexes [303]. This leads to fibrin deposition forming a matrix that is invaded by fibroblasts with the formation of extracellular matrix (ECM). This ECM can still be completely degraded by the proenzymes of matrix metalloprotease (MMP), leading to normal healing. However, if this process is inhibited by tissue inhibitors of MMPs, peritoneal adhesions may be formed [304]. Generally, the balance between plasminogen activators and plasminogen inhibitors is crucial in determining normal healing or adhesion formation [305]. If fibrinolysis does not occur within 5 to 7 days of peritoneal injury, the temporary fibrin matrix persists and gradually becomes organized with collagen-secreting fibroblasts. This process leads to peritoneal adhesion formation [301, 306] and growth of new blood vessels mediated by angiogenic factors [307].

Prevention of post-surgery tissue adhesion may be based on pharmacological agents [308] and/or physical barriers. Pharmacological agents with anti-adhesion properties include fibrinolytic agents such as streptokinase [309], anticoagulants such as low molecular weight heparin (Enoxaparin-Na) [310], anti-inflammatory agents [311], antihistamines [312], broad-spectrum antibiotics chiefly cephalosporins [309], anti-proliferative drugs such as camptothecin [313] and antioxidants such as Vitamin E [314] and methylene blue [315]. However, several factors may limit the use of pharmacological agents in preventing tissue adhesion. Firstly, ischaemic sites liable to adhesion formation are cut off from systemic drug delivery. Secondly, the peritoneum rapidly absorbs and reduces the efficacy of intraperitoneally administered agents. Thirdly, anti-adhesion agents may affect normal wound healing [128].

Apart from pharmacological agents, mechanical barriers may prevent postoperative peritoneal adhesion by keeping peritoneal surfaces separated during the 5-7 day required for peritoneal re-epithelialization [308]. They prevent contact between the damaged serosal surfaces for the first few critical days. An ideal barrier should be biodegradable, safe, non-inflammatory and non-immunogenic. It should also withstand the critical re-mesothelialisation phase, stay in place without sutures or staples, remain active in the presence of blood and be rapidly and easily applied [316]. To date, many commercially available anti-adhesion barriers are based on hydrogels such as a combination of hyaluronic acid and carboxymethyl cellulose [317] and oxidized-regenerated cellulose which also assists in the control of surgical bleeding [318]. In addition to gels, fabric-based products such as absorbable satin-like fabric made from oxidized regenerated cellulose is commonly used in open surgery for reducing postoperative adhesions after hemostasis [319]. Further, cast films have been widely used as anti-adhesion barriers [320, 321].

A combined approach based on the concomitant use of physical barriers and pharmacological agents may greatly enhance the effectiveness of tissue adhesion management. In this context, drug-eluting physical barriers would mechanically prevent tissue adhesion and improve the presentation of the anti-adhesion pharmacological agents by providing prolonged, localized and temporally controlled delivery of the agent to the injured sites [131]. For instance, Sahin and Saglam [322] used a combination of carboxymethyl cellulose sodium and heparin at laparotomy, demonstrating greater activity of the combination in reducing adhesion formation compared to heparin alone. Gong *et al* [323] formulated biodegradable doxorubicin-loaded poly(ethyleneglycol)–poly(ε-caprolactone)–poly(ethylene glycol) (PECE) copolymer micelles in water, which turned instantly into gel at body temperature as a result of micellar aggregation. The loaded micelles were used to improve intraperitoneal chemotherapeutic effect and prevent postsurgical peritoneal adhesions simultaneously in a mouse model for postsurgical residual tumors and peritoneal adhesions. Membranes made of biodegradable polymers such as polyhydroxybutyrate-co-hydroxyvalerate (PHBV) were reported to deliver streptokinase continuously and to reduce the extent and severity of tissue adhesions [324]. More recently, nanofibers were shown to reduce post-surgery adhesion by acting as a physical barrier as well as a local drug delivery vehicle [30, 47, 131]. Zong *et al* [131] demonstrated effective reduction of peritoneal adhesions in a rat model by using PLGA/PEG-PLA nanofibrous membranes impregnated with 5 % cefoxitin sodium.

The objective of this chapter of the thesis was to develop a new combination anti-adhesion suppression approach based on the literature reported tissue anti-adhesion properties of methylene blue (MB) as a pharmacological agent with antioxidant and antimicrobial properties and PHB-based nanofibrous and cast membranes as physical barriers. MB was reported to exert a tissue anti-adhesion effect by reducing the initial inflammatory response, thereby blocking an oxidative stress-dependent decrease in peritoneal fibrinolytic activity [268]. As antioxidant, MB inhibits the generation of oxygen radicals (e.g. superoxide, peroxides, and hydroxyl radicals) [269]. It also exerts antibacterial activity that could be effective in reducing infection-induced adhesions [325]. However, MB undergoes rapid degradation via intra-abdominal proteases such as tissue plasminogen activator (tPA), a major component of the peritoneal fibrinolytic system [24]. PHB was thought to be a suitable polymer for tissue anti-adhesion applications because of the physicomechanical properties of PHB-based membranes such as mechanical strength and lightness. The tissue adhesion suppressive effect of MB-loaded PHB-based nanofibers and cast membranes of different polymer composition and structural features was assessed in a cecal abrasion model in rats. Anti-adhesion efficacy was assessed macroscopically, microscopically and histopathologically.

## 2. Materials and Methods

### 2.1. Materials

#### Chemicals

- Methylene blue (MB) (Aldrich chemical co. Ltd., England)
- Polyhydroxybutyrate Poly(R-3-hydroxybutyrate) (PHB, 250 kDa, Nantian Co. Ltd., Jiangsu, China)
- Polyethylene glycol 4000 (PEG 4000) (Fluka AG, Buchs SG, Switzerland)
- Span 80 (Guang dong Guanghua Chemical Factory Co. Ltd., China)
- Chloroform (Sigma-Aldrich co. Ltd., England)
- Ethanol Absolute (Sigma-Aldrich, Germany)
- Thiopental® (Thiopentone sodium injection)Sandoz, Germany
- Savlon® (cetrimide-chlorhexidine solution), Novartis, Egypt.

#### Animals

The experimental animals used were young female *Wistar* rats of 2 month-age and weighing (130 ± 10 g). Rats were obtained from the animal house of the Faculty of Pharmacy, Alexandria University. The rats were kept on a diet providing the daily needs of nutrients and water. The rats were housed individually in cages. They were maintained in a temperature and humidity controlled environment at the animal house of the Faculty of Pharmacy, Alexandria University.

All animal procedures were adopted in accordance with the Guidelines for Ethical Conduct in the Care and Use of Research Animals developed by the American Psychological Association (APA) Committee on Animal Research and Ethics (CARE). Human care of all animals was strictly followed throughout the *in vivo* study.

### 2.2. Equipment

- Electrospinning apparatus equipped with High Voltage DC Power Supply(P3508, Raymax, Canada ) and a syringe pump (101, KD scientific, USA )
- Vortex mixer (VM-300, KK ,USA )
- Adventurer sensitive electrical digital balance (Ohause Corp. Pine Brook, NJ, USA).
- Hot plate magnetic stirrer (IP 21, IKA, Staufen, Germany)
- UV-Visible Spectrophotometer (T80 UV/ Vis PG Instruments Spectrophotometer. ltd, England).
- Digital camera, 12 mega pixels, 5X optical zoom (ES70, Samsung Co, South Korea).
- Scanning electron microscope (JSM-5300, JEOL, Japan).
- Ion sputtering coater (JFC-1100E, JEOL, Japan).
- Light microscope with digital camera (CX41, Olympus America Inc., USA).
- Micrometer (IP 65, Mitutoyo Manufacturing, Tokyo, Japan)
- Micropipettes (Comecta, Spain).
- Sterile silk braided non-absorbable sutures 3-0 with 8/3 circle reverse cutting needle, USP ( DemeTech, USA)

## 2.3. Methods

### Treatment of induced post-surgical peritoneal adhesions in rats using PHB biomaterials

### 2.3.1. Preparation of anti-adhesion PHB membranes (nanofibers and cast films)

A total of seven PHB-based membranes (five nanofibrous membranes and two cast films) were used in the study. The properties of these membranes are shown in Table 8.

Plain NFs made of PHB ($NF_1$) or a 3: 2 PHB/PEG blend ($NF_2$) and their corresponding MB-loaded membranes ($NF_3$ and $NF_4$ respectively) were prepared by emulsion electrospinning as described in chapter 1. Sheets $\approx$ 0.35 mm-thick were cut into 3 x 3 $cm^2$ samples weighing $\approx$65 mg each. For the preparation of the $NF_5$ membranes, 3 x 3 $cm^2$ squares of $NF_3$ were additionally loaded with MB by deposition of 570 µl of 0.4% MB solution (for good distribution) layer by layer using a micro-syringe on the surface of the nanofibrous membrane. Each layer was allowed to be absorbed by the NFs and was completely air dried away from light before application of subsequent layers.

Plain PHB films were prepared by casting a chloroformic solution of PHB (12% w/v) and Span 80 (6.6% w/w) with the same composition as the polymer organic phase used for the emulsion electrospinning of plain PHB nanofibers samples ($NF_1$). MB-loaded PHB films ($CF_2$) were prepared by casting an emulsion consisting of 12% w/v of PHB solution in chloroform containing Span 80 (6.6% w/w) as the oil phase and 2% w/v MB solution as the aqueous phase. The oil: water phase volume ratio was 20:1. The emulsion was prepared by vortexing and poured into Petri dishes that were covered to allow for controlled drying of the solvent. For the preparation of cast films with additional MB surface loading, samples of MB-embedded casted films ($CF_2$) $\approx$ 0.1 mm-thick were cut into 3 x 3 $cm^2$ squares weighing $\approx$ 40 mg. These were further loaded with MB by multilayer deposition of equal volumes (113 µl) of 1% MB solution on both surfaces of the membrane; each layer was allowed to dry before deposition of subsequent layers. The casted films were kept in a desiccator. All test membranes were examined by SEM for the fine features of the surface.

**Table 8: Types and properties of PHB-based membranes used in the study**

| Membrane code | Type | Polymer composition | MB loading | MB content/ membrane, mg/mg |
|---|---|---|---|---|
| **$NF_1$** | Nanofibers | PHB | - | - |
| **$NF_2$** | " | PHB/PEG (3: 2) | - | - |
| **$NF_3$** | " | PHB | Encapsulation | 0.325 mg/ 65 mg |
| **$NF_4$** | " | PHB/PEG (3: 2) | Encapsulation | 0.325 mg/ 65 mg |
| **$NF_5$** | " | PHB | Encapsulation + surface deposition | 2.6 mg/ 65 mg |
| **$CF_1$** | Cast emulsion film | PHB | - | - |
| **$CF_2$** | " | PHB | Embedding + deposition on both surfaces | 2.6 mg/ 40mg |

### 2.3.2. Pre-operational care techniques:

The surgical table and the operating board were disinfected with Savlon® (cetrimide-chlorhexidine) solution diluted 1 in 10. Disinfection was performed for each surgery. The surgical instruments were sterilized by boiling for 15 minutes in Savlon® (cetrimide-chlorhexidine) solution diluted 1 in 10. The surgical instruments were left to cool in the dilute chlorhexidine solution. The antiseptic solution was washed away using 70% alcohol. A new set of surgical instruments was used for each animal.

The rat was weighed and anesthetized with thiopentone sodium (50 mg/kg body weight) administered by intra-peritoneal injection. The abdominal area of the animal was clipped with a pair of scissors (other than those used in surgery). The skin was prepared by scrubbing with 70% ethanol.

### 2.3.3. Surgical protocol and induction of peritoneal adhesion:

The procedure was adapted from Yang *et al* [49]. A longitudinal incision (3 cm long) was made on the midline of the abdominal wall and the abdomen was opened. The cecum was observed and exposed, then gently abraded using a blade at all surfaces until it lost its shine, and hemorrhagic points became visible without perforation. The opposing abdominal wall was scraped with a scalpel blade until the surface was disrupted. The cecum was then returned to its anatomic position facing the denuded abdominal wall. The abdominal wall and skin were sutured using sterile silk braided non-absorbable sutures 3-0 with 8/3 circle reverse cutting needle. The procedure is illustrated in Figure 31.

### 2.3.4. Study protocol

The study involved a total number of 60 female *Wistar* rats and was conducted in two subsequent experiments, A and B involving seven and five groups of rats respectively (Table 9). Each group included five rats. The first experiment (Experiment A, rat groups 1-7) had two objectives, firstly to assess the effect of polymer composition on the anti-adhesion effect of test membranes (PHB, $NF_1$ *vs* PHB/PEG, $NF_2$) as physical barriers; secondly, to assess the effect of MB at a dose 2.5 mg/kg on the anti-adhesion effects of both MB-eluting PHB membranes ($NF_3$ *vs* $NF_1$) and PHB/PEG membranes ($NF_4$ *vs* $NF_2$) as medicated physical barriers using MB solution providing 2.5 mg/kg dose (MB-2.5) as control instilled in defected tissues. Sham operated rats (Sham) were used as negative control and untreated rats (UT_A) were used as positive controls.

Based on the findings of experiment one, the second experiment (B, Table 9) was conducted to enhance the anti-adhesion effect. The objective of experiment B was two-fold: firstly, to assess the effect of increasing the MB load of PHB NFs ($NF_5$, Table 8) to provide a MB dose of 20 mg/kg using a free MB solution at the same dose (MB-20) and untreated rats (UT-B) as controls; secondly, to compare the effect of a cast film with the same polymer composition and MB load as an unstructured barrier ($CF_2$) with that of MB-eluting PHB NFs ($NF_5$) as a nanofibrous barrier using plain PHB cast film ($CF_1$) as control.

**Table 9: Experimental groups of rats and treatments under study**

| Experiment | Rat group | Code | Treatment with MB solution, NFs or film | Delivered MB dose, mg/kg |
|---|---|---|---|---|
| A | 1 | Sham | One ml sterile saline instilled i.p. (-ve control) (sham operated) | - |
| | 2 | UT-A | Untreated (+ve control) | - |
| | 3 | $NF_1$ | Plain PHB NFs | - |
| | 4 | $NF_2$ | Plain PHB/PEG NFs | - |
| | 5 | MB-2.5 | One ml 0.325 mg/ml MB solution i.p. | 2.5 |
| | 6 | $NF_3$ | MB-loaded PHB NFs | 2.5 |
| | 7 | $NF_4$ | MB-loaded PHB/PEG NFs | 2.5 |
| B | 8 | UT-B | Untreated (+ve control) | |
| | 9 | MB-20 | One ml of 2.6 mg/ml MB solution | 20 |
| | 10 | $NF_5$ | MB-loaded PHB NFs by encapsulation and surface deposition | 20 |
| | 11 | $CF_1$ | Plain PHB casted film | - |
| | 12 | $CF_2$ | MB-loaded PHB casted film by embedding and surface deposition | 20 |

*Peritoneal adhesion was induced in all groups by surgical abrasion except the sham operated group (the cecum was just exposed with no surgical abrasion).

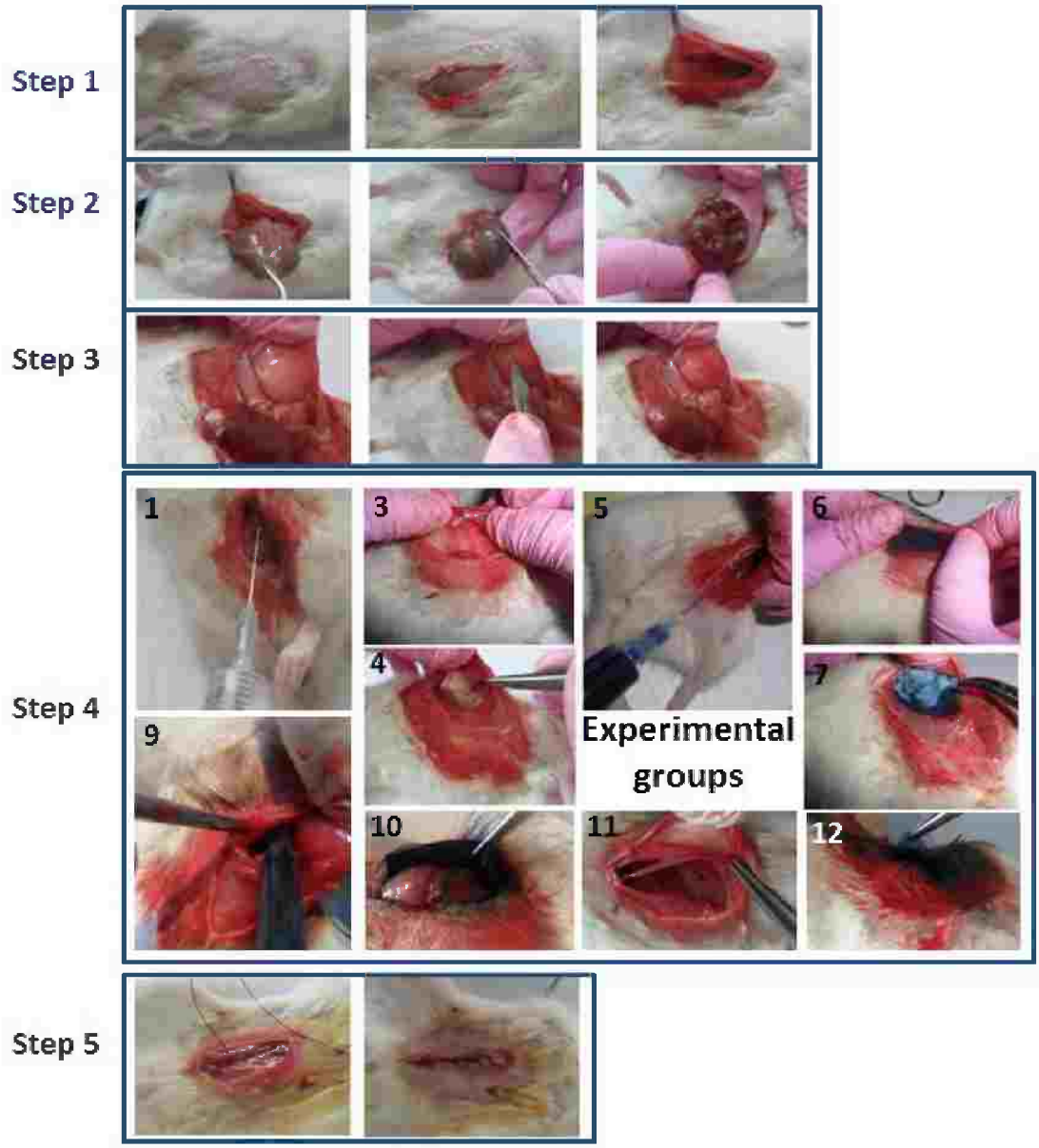


**Figure 31: Steps of surgical procedure for induction of peritoneal adhesion in young female *Wistar* rats.**

**Step 1**: A longitudinal incision (3 cm long) was made on the midline of the abdominal wall
**Step 2:** The cecum was gently abraded until hemorrhagic points became visible without perforation
**Step 3:** The opposing abdominal wall was scraped
**Step 4:** Animal groups treated as described in Table 9
**Step 5:** The abdominal wall and skin were sutured

### 2.3.5. Assessment of the anti-adhesion properties of test membranes:

The anti-adhesion properties of the test membranes were assessed macroscopically, histologically and by total and differential white blood cell count.

#### 2.3.5.1. Macroscopic evaluation:

The adhesion prevention effectiveness of the membranes was assessed by grading adhesions according to extent, type and tenacity of adhesions using a reported two-scaling system [47, 130, 326-328] as shown in Table 10.

**Table 10: Description of different peritoneal adhesion scores using two-scaling system**

| Score | Adhesion characteristics | | |
|---|---|---|---|
| | Extent | Type | Tenacity |
| 0 | - | - | - |
| 1 | Filmy | Transparent, avascular | Adhesions fall apart |
| 2 | Mild | Opaque, translucent, avascular | Adhesions lysed with traction |
| 3 | Moderate | Opaque, capillaries present | Adhesions sharply dissected |
| 4 | Severe | Opaque, larger vessels present | Adhesions not dissectible without damaging organs |

#### 2.3.5.2. Histological examination

Adhesion bands and the cecum tissue were extracted from surrounding tissues, fixed in 10% formalin and immersed in paraffin. Several paraffin sections were made by microtoming. These sections were stained using Haematoxylin and Eosin (H & E) for general analysis and Masson's trichrome for assessment of collagen formation

#### 2.3.5.3. Total and differential white blood cell count

Quantitation of the absolute numbers of circulating leukocytes was determined in terminal blood obtained by heart puncturing at day 14 post surgery. One ml blood was transferred to EDTA tube. The blood was well mixed without shaking and analyzed on the same day. The total and differential white circulating blood cell count/µl was determined using an automatic cell counter (flow cytometer).

### 2.3.6. Characterization of retrieved PHB membranes

Retrieved membranes were characterized for morphological changes and MB content.

#### 2.3.6.1. Morphological examination macroscopically and by scanning electron microscopy (SEM)

Retrieved membranes were examined for macroscopical change in thickness before and after implantation. Membranes were also examined by SEM with accelerating voltage of 25 kV. The samples were fixed in buffered 10% formalin. The samples were dehydrated by successive treatments with 30, 50, 70, 80 and 90% ethanol. Samples were dried then coated with gold using an ion sputtering coater and examined by SEM at two magnification powers X1000 and X2000. Cross sections of fibers were examined as well.

#### 2.3.6.2. MB content of PHB membranes retrieved from abdominal cavities at day 14

The amount of MB remaining in retrieved MB-loaded nanofibrous mat from group A was determined after multiple extraction by soaking in 5 ml absolute ethanol in well-closed screw capped tubes. Complete MB extraction was verified spectrophotometrically and by complete bleaching of NFs. MB concentration in each ethanolic solution was calculated using a pre-constructed calibration curve of MB in absolute ethanol at $\lambda$max 654 nm and the amount of MB remaining was calculated. The % MB remaining in retrieved membranes was determined using the following equation:

$$\% \text{ Remaining MB} = \frac{\text{Remaining MB content}}{\text{Intial MB content}} x\ 100$$

### 2.3.7. Statistical analysis

Quantitative data obtained in each experiment were subjected to statistical analysis using a one-way analysis of variance test followed by a post Newman-Keuls test with $P \leq 0.05$ denoting significance. Analysis was performed using GraphPad Prism 5 © software.

## 3. Results and discussion

In chapter one of the thesis, electrospun MB-loaded nanofibers were developed using PHB as a polymer matrix. These NFs potentially exert multiple functions based on the combined local effects of NFs as a nanofibrous membrane or scaffold, the NFs physicochemical characteristics conferred by PHB and the multiple biological effects of MB. The pharmaceutical attributes of these NFs were modulated to enhance their performance, particularly controlled MB release. Accordingly, the MB-loaded PHB NFs developed may offer potentials in different biomedical applications where multifunctionality of this medicated nanofibrous matrix is required. This will be the subject of chapters 2 to 4 of the thesis.

In chapter 2, the potentials of MB-loaded PHB-based membranes as physical barriers to suppress post-surgical peritoneal adhesions in a rat model were investigated. The contribution of compositional variables such as polymer composition (PHB *vs* PHB/PEG), MB loading (plain *vs* MB-loaded NFs) and MB dose (2.5 mg/kg *vs* 20 mg/kg body weight) and structural difference of the polymer matrix (nanofibers *vs* cast film) was investigated for a better assessment of the individual anti-adhesion effects. Interest in this study has been driven by controversies in the literature regarding the function of MB and different types of physical barriers in tissue anti-adhesion applications. Several studies revealed that MB does exert anti-adhesion effect [268, 269, 329, 330]. However, a recent report demonstrated that MB would increase the degree of peritoneal adhesion [331]. As far as physical barriers are concerned, both cast films [133, 320, 321, 332, 333] and nanofibrous membranes made of different types of polymers [30, 47, 49, 130-132] were used as tissue anti-adhesion barriers with demonstrated efficacy in comparison with commercial products in many instances. However, as these studies were carried out under different experimental conditions, comparison between results obtained may be difficult. This justified a comparison of the tissue anti-adhesion effect of NFs and cast membranes under similar conditions.

The rat peritoneum was selected for the study as the peritoneum is one of the most common sites for tissue adhesion after abdominal surgery. All rats survived the study with no evidence of toxicity. The abdominal cavity of the animals was examined at the end of the 14 day-study for the development of adhesions. These were assessed using a grading scheme to judge the extent, type and tenacity of adhesions. Moreover, adhesion bands and sites of adhesion in the cecum were assessed histopathologically. Furthermore, differential WBCs count in peripheral blood was assessed.

### 3.1. Experiment A: Assessment of the anti-adhesion properties of PHB-based nanofibers and MB solution at a dose of 2.5 mg/kg:

In this experiment, the tissue ant-adhesion effects of PHB-based NFs and cast membranes were investigated using a MB dose of 2.5 mg/kg as entailed by MB load of the test NFs (Chapter 1). Although this dose is smaller than those reported for MB solution in tissue anti-adhesion studies [268, 270, 271], it was considered acceptable for a MB delivery system allowing to reduce drug loss at the site of application. Moreover, this MB dose was larger than that used in

adhesion prevention in gynecological applications [334] and sufficient for exerting an antibacterial effect (Chapter 1), of importance in preventing abdominal tissue adhesions.

### 3.1.1. Macroscopic assessment:

Figure 32 shows representative digital photographs of the abdominal cavity of rats of groups 1-7 at the end of the experiment in comparison with normal viscera. Different degrees of adhesion were observed in test rats, with more pronounced adhesion formation in untreated rats (UT-A), rats treated with plain PHB/PEG NFs ($NF_2$) and those treated with MB solution 2.5 mg/kg (MB-2.5). The degree of peritoneal adhesion and characteristics of adhesion bands are fully described in Table 11. Adhesion scores ± SD are shown in Figure 33. Scores were subjected to statistical analysis to evaluate the significance of difference in extent and severity of adhesions between different treatments. One way ANOVA indicated no significant difference ($p<0.05$) between groups treated with plain PHB/PEG NFs ($NF_2$), MB solution-2.5 mg/kg (MB-2.5) and the untreated group (UT-A) regarding the type, extent and tenacity of peritoneal adhesions. However, treatment with plain PHB NFs ($NF_1$), MB-loaded PHB NFs ($NF_3$) and MB-loaded PHB/PEG NFs ($NF_4$) resulted in 30, 25 and 25 % reduction respectively in adhesion type and extent relative to the untreated group (60% adhesion). The difference was statistically significant ($p<0.05$). Furthermore, MB-loaded PHB NFs ($NF_3$) resulted in a significant 35% reduction in adhesion tenacity score ($p<0.05$) in relation to the untreated control group. It was worth-noting that MB was completely released from PHB/PEG NFs ($NF_4$) while it was noticeably retained by the more hydrophobic PHB NFs ($NF_3$) (Figure 32) which was consistent with *in vitro* MB release data (Chapter 1). In general, the maximum adhesion suppression effect observed in experiment A treatments was 30 % relative to the control, for extent and type, achieved by plain PHB NFs, and 35% for tenacity, achieved by MB-PHB NFs.

Macroscopic examination coupled with adhesion scores indicated that the polymer composition affected the tissue anti-adhesion effect of PHB-based NFs as well as the contribution of encapsulated MB to the effect. In brief, PHB NFs were more effective than the more hydrophilic PHB/PEG NFs in reducing tissue adhesions and MB loading did not affect the anti-adhesion effect of PHB NFs though it enhanced that of PHB/PEG NFs.

For a better understanding of the effect of polymer composition on reduction of tissue adhesion, PHB and PHB/PEG membranes retrieved from the abdominal cavity of rats at the end of the study were compared macroscopically and by SEM. Digital photographs (Figure 34) showed obvious swelling associated with increased porosity and thickness of the PHB/PEG membrane. The matrix thickness measured before implantation and 14 days post-surgery was 0.34 µm ± 0.04 and 0.51 µm ± 0.12 respectively for plain PHB NFs (1.5-fold increase) while it was 0.31 µm ± 0.05 and 2.25 µm ± 0.55 respectively for plain PHB/PEG NFs (7.25-fold increase). Increased thickness and modified internal NFs architecture and porosity were evidenced by SEM of cross sections of the retrieved membrane (Figure 34). Moreover, SE micrographs of the NFs matrices (Figure 35a and b, upper panel) showed much more extensive cell infiltration into the porous PHB/PEG NFs matrix compared to surface cell growth on plain PHB NFs. Enhanced cell proliferation on PHB/PEG NFs can be driven by the higher hydrophilicity of the matrix, its swollen internal structure and greater porosity, induced by leaching of PEG. It has been reported that an optimum degree of intermediate hydrophilicity may

be needed for cell attachment and proliferation on polymeric scaffolds. Spasova *et al* [335], using polyethylene polymer surfaces with gradient wettability, demonstrated that endothelial cells adhered more onto the positions with intermediate hydrophilicity than onto the position with high or low hydrophilicity, though cell adhesion force was greater on hydrophilic sites. Further, cell growth was reported to proceed on NFs made of a poly(L-lactide) (PLLA)/polyethylene glycol (PEG) polymer blend (90: 10, 80: 20 and 70: 30 ratios) with more long-term growth upon increase of the PEG proportion, as a result of more adequate hydrophilicity. In addition to the PEG hydrophilicity effect observed in the present study, leaching of PEG from the blend PHB/PEG polymer matrix resulted in increased porosity with a change in internal architecture of the matrix (Figure 35b). Similarly, a porogenic effect has been reported upon leaching of polyethylene oxide (PEO) from a polycaprolactone/PEO fibrous mat matrix [336]. Increased porosity may generate gaps within the fibrous structure resulting in cell infiltration and in growth into the fibers. Interestingly, using PEG to modulate hydrophilicity of scaffolds made of copolymers of PEG and hydrophobic polymers reduced cell adhesion and growth on the scaffold surface [49].

Results obtained in the study coupled with literature data suggested that the hydrophilic polymer moiety used to modulate the hydrophilicity of polymer physical barriers intended for tissue ant-adhesion applications should be conjugated to the polymer backbone to preclude leaching. The high surface hydrophilicity and mobility of the hydrated PEG chains exposed on the surfaces, prevent cell attachment and proliferation [337].

Regarding the effect of MB solution on tissue adhesion, Figures 32 and 33 showed that instillation of MB solution into the injured tissue of rats did not significantly reduce tissue adhesion 14 days post-surgery, though cell growth on the surface of both MB-loaded PHB NFs and MB-loaded PHB/PEG NFs was obvious (Figure 35). Despite literature controversies, the anti-adhesion effect of MB was reported to be dose-dependent [270]. Limited reduction of abdominal adhesions in the present study can be attributed to the relatively low dose of MB used (2.5 mg/kg). Possible enhancement of MB tissue anti-adhesion effect by encapsulation in NFs as a controlled delivery system allowing reduction of loss was assessed.

Results for MB encapsulated in PHB-based NFs indicated that treatment with MB-loaded PHB NFs did not significantly change the adhesions extent and tenacity score ($p>0.05$) while treatment with MB-loaded PHB/PEG NFs resulted in a significant reduction in extent and type score ($p<0.001$) (Figures 32 and 33). The enhanced tissue anti-adhesion effect of MB-eluting PHB/PEG NFs can be attributed to the relatively fast release of MB from the polymer matrix as a result of leaching of PEG and fluid penetration into the matrix (as demonstrated in the *in vitro* release study in chapter 1). In the absence of PEG (PHB NFs), MB was retained in the matrix as evidenced by the blue colour of MB-loaded PHB/PEG NFs in the abdominal cavity at the end of the study (showed in Figure 32). This probably explains the statistically insignificant difference in the anti-adhesion performance of plain PHB and MB-loaded PHB NFs. Difference in MB release was verified by determination of the amount of MB retained by both NFs matrices 14 days post implantation. The % MB retained was $7.3 \pm 1.7$ % and $81.8 \pm 6.1$% for PHB/PEG NFs and PHB NFs respectively. Fast initial release of pharmacological agents, particularly those with antimicrobial activity is necessary as in most cases infections occur within the first few hours after surgery occur. Early availability of the antimicrobial agent at the site of abdominal surgery

supports prevention of infections and the abdominal adhesions triggered by microorganisms at this site [47]. Accordingly, results suggested that the activity of MB was affected by the polymer composition of the NFs matrix. Despite enhanced tissue adhesion by PHB/PEG NFs, burst release of MB resulted in a significant enhancement of the performance of the medicated PHB/PEG matrix. On the other hand, incorporation of MB in a controlled delivery system enhanced its tissue anti-adhesion effect, probably as a result of effect prolongation. Similarly, embedding omidazole, a metronidazole derivative, in electrospun nanofibers reduced abdominal adhesions in rats and synergistically enhanced the healing process [47]. Combined experimental and literature reported data point to the importance of pharmaceutical presentation of anti-adhesion drugs provided that relatively fast release is granted during the early phase of treatment.


**Figure 32: Representative images show normal viscera, sham operated and groups of peritoneal adhesion model.**

*Adhesion of cecum to abdominal wall or the implanted membrane (white arrows) and adhesion bands (black arrows)

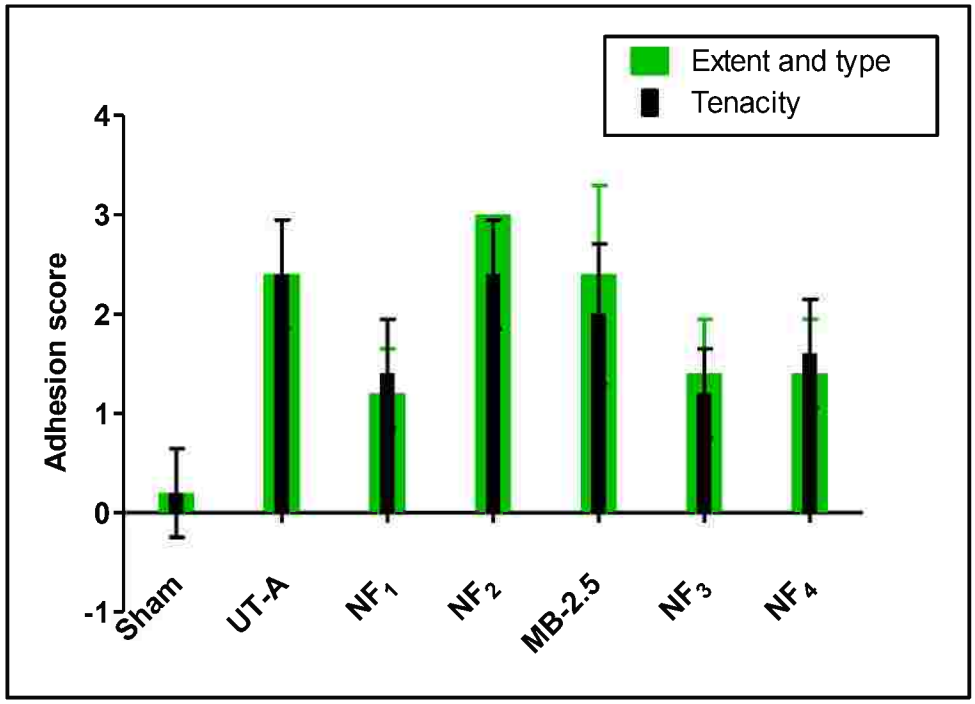


**Figure 33: Scores for adhesion extent, type and tenacity of different rats groups of experiment A.**

**Table 11: General description of peritoneal adhesion of different rat groups of experiment A.**

| Rat group | Code | Description of peritoneal adhesion/ Extent, type and tenacity[47, 130, 326-328] |
|---|---|---|
| 1 | Sham | Mainly free from adhesion |
| 2 | UT-A | Moderate opaque adhesions with capillaries. Sharp / gentle dissection |
| 3 | $NF_1$ | Mild opaque avascular adhesions Gentle dissection |
| 4 | $NF_2$ | Moderate opaque adhesions with capillaries Gentle/sharp |
| 5 | MB-2.5 | Moderate opaque avascular adhesions. Sharp / gentle dissection |
| 6 | $NF_3$ | Mild opaque adhesions, avascular, Gentle dissection |
| 7 | $NF_4$ | Mild opaque , avascular adhesions, Gentle dissection |

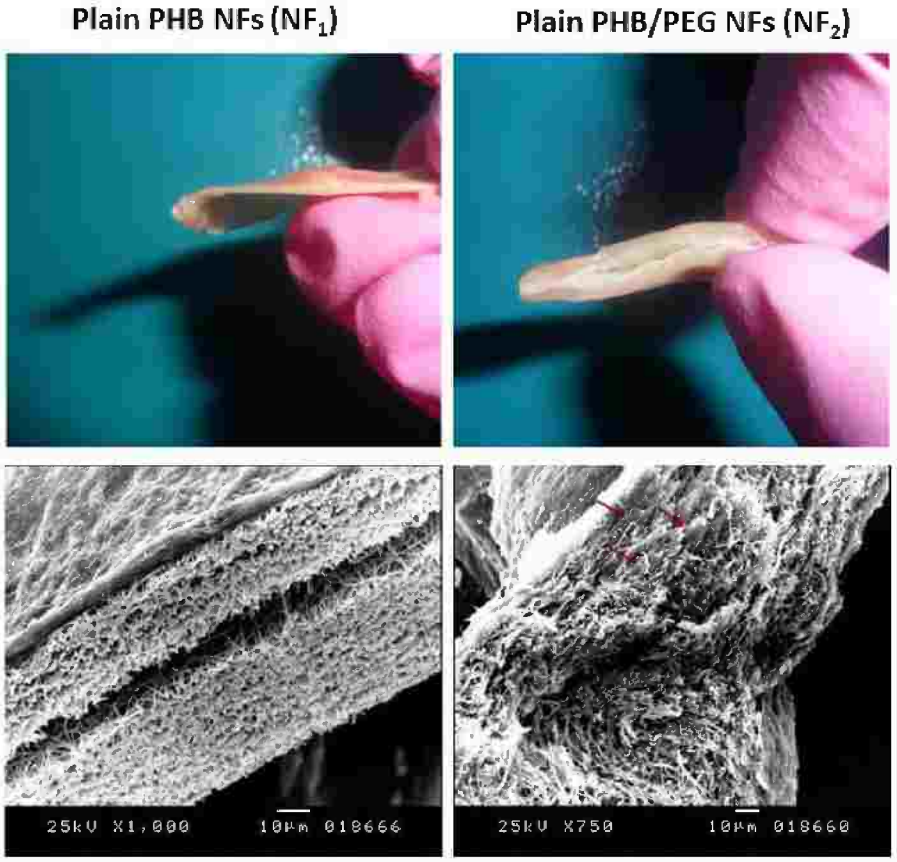


**Figure 34: Digital photographs (upper panel) and SEM (lower panel) of samples of plain PHB NFs ($NF_1$) and plain PHB/PEG NFs ($NF_2$) retrieved after implantation for 14 days in the peritoneal cavity of rats.**

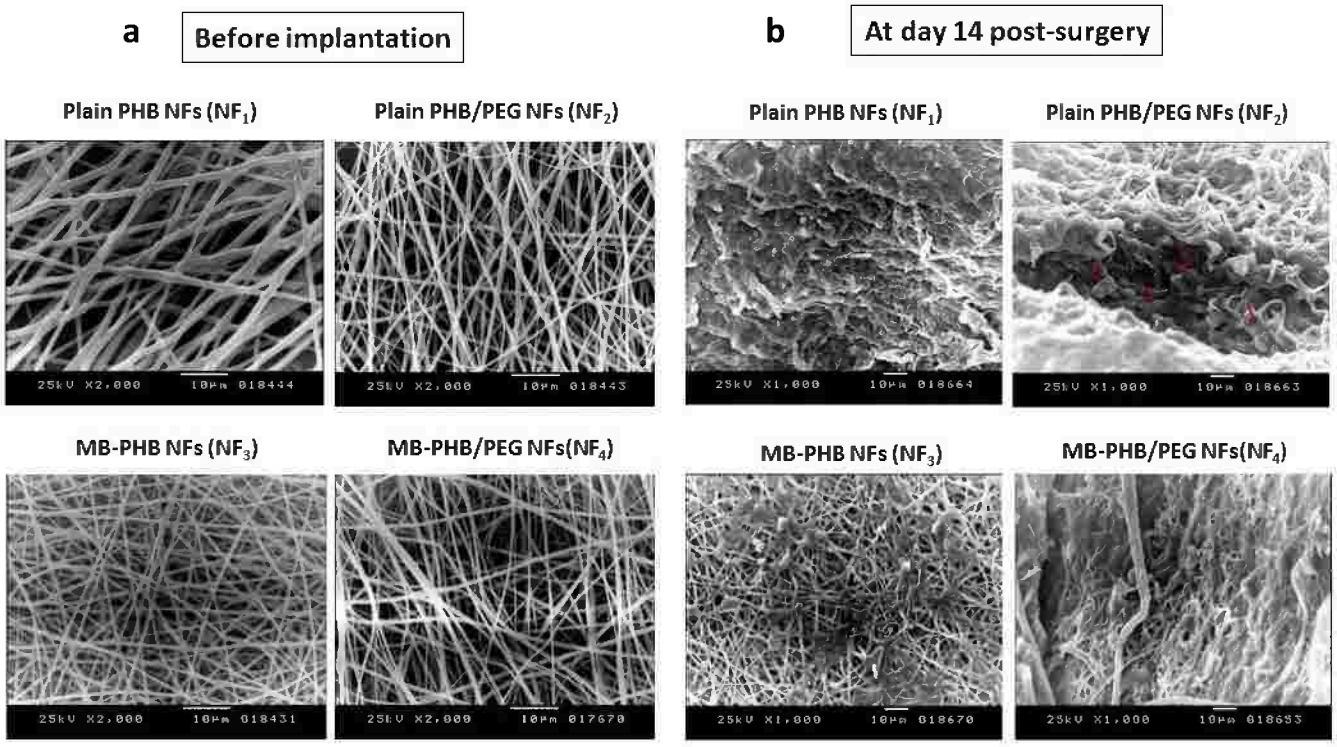


**Figure 35: SEM of samples of plain PHB NFs ($NF_1$) and PHB/PEG NFs ($NF_2$) (upper panel) and their MB-2.5 loaded counterparts (lower panel); a) before implantation and b) after implantation for 14 days in the peritoneal cavity of rats.**

### 3.1.2. Histopathological examination

This was performed on biopsies from the cecal wall at the site of abrasion and adhesion bands for different treatments in Experiment A (Table 9). Results for biopsies from normal cecal tissue as control and for biopsies from cecal tissue and adhesion bands post- surgery are shown in Figures 36 and 37 respectively.

Biopsies taken from control untreated rats (UT-A) and the different treatment groups showed minimal repair of the injured serosa and muscle layer. This was associated with acute inflammation with leukocytic infiltration, edema and ulceration of the cecum muscle layer. Edema and infiltration of leukocytes extended to the submucosal layer, where dilation and congestion in the blood vessels could be observed. Newly formed adhesion tissue containing a thick layer of fibroblasts and collagen fibers could be seen between the abdominal wall and the cecum wall. Biopsies from the adhesion bands showed persistent angiogenesis with well-developed blood vessels, infiltration of inflammatory cells and compact arrangement of collagen fibers.

For plain PHB NFs ($NF_1$), biopsies from adhesion sites showed continuous muscle layer and enhanced healing of the cecal wall. Minor focal edema and infiltration of leukocytes in the muscle layer were seen. This was associated with a decreased tendency for adhesion. Biopsies from the adhesion bands showed fewer newly formed blood vessels and the collagen fibrils were loosely arranged with mild infiltration of leukocytes. However, histopathological findings for plain PHB/PEF NFs ($NF_2$) were not different from those of the untreated group.

Treatment of the abrasion site with MB solution 2.5 mg/kg (MB-2.5) resulted in partial repair. Acute inflammation with leukocytic infiltration, edema and ulceration of the cecum muscle layer was still seen, yet it was less intense than that observed in the untreated group. Focal edema and infiltration of leukocytes extended to the submucosal layer, which showed congestion and dilation of the blood vessels. Biopsies from the adhesion bands showed persistent angiogenesis and less compact arrangement of collagen fibers compared to the untreated group.

Loading of plain PHB NFs and PHB/PEG NFs, ($NF_3$ and $NF_4$ respectively) with MB enhanced healing of the cecal wall in both cases, though a more continuous muscle layer could be observed with $NF_4$. Edema and infiltration of leukocytes in the muscle layer and submucosa were reduced and there was a decreased tendency for adhesion. Adhesion bands for MB-loaded PHB NFs ($NF_3$) were comparable to those developed by their plain counterpart ($NF_1$). Biopsies from the adhesion bands for rats treated with $NF_4$ showed fewer newly formed blood vessels and the collagen fibrils were loosely arranged. Fewer fibroblasts and leukocytes were observed compared to the adhesion bands of the untreated group.

Despite insufficient suppression of tissue adhesion reduction generally achieved in experiment A, main findings indicated that plain hydrophobic NFs as a physical barrier exerted a significant tissue adhesion reduction effect. Further, encapsulation enhanced the tissue anti-adhesion effect of MB, though the effect could be further enhanced by increasing the MB dose.

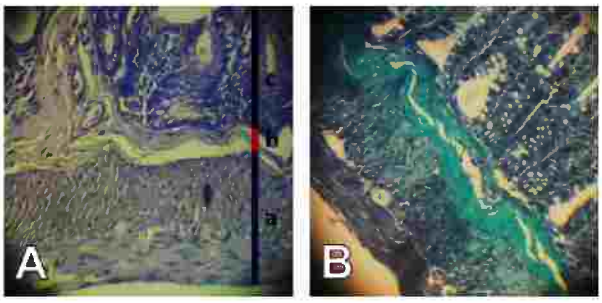


**Figure 36: Normal rat cecal wall: Photo (A): Section in the wall of normal rat cecum stained with H & E stain (magnification 100X) showing the normal tissue architecture of the cecal wall. Note the uniformity of the muscle layer (a), submucosa (b), and mucosa (c). Photo (B): Masson's trichrome stain (magnification 100X) showing normal collagen fibers in the wall of the cecum.**

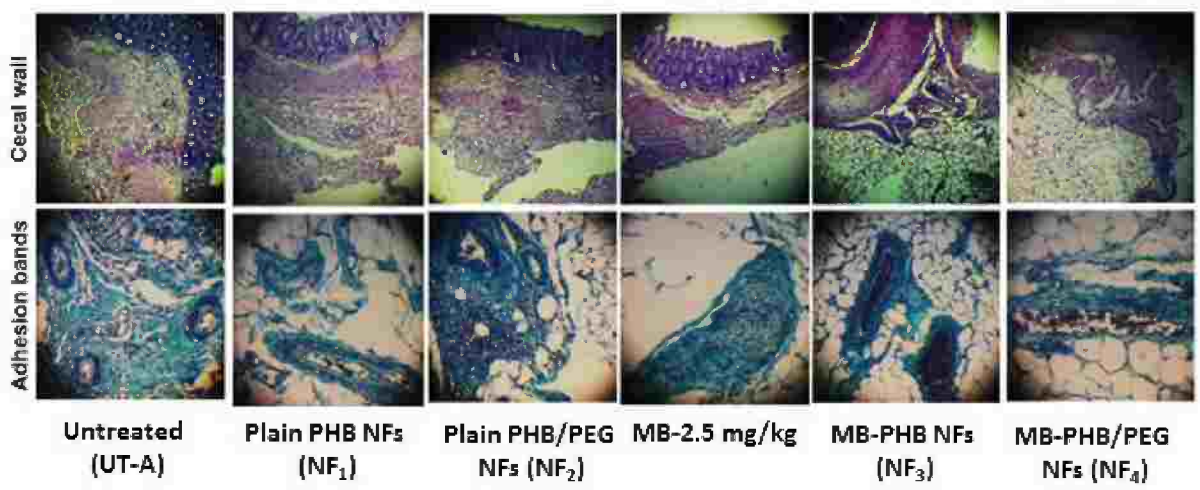


**Figure 37: Upper panel: photomicrographs for sections form biopsies of the cecal wall of different treatment groups (Experiment A) stained with H & E (magnification 40X) demonstrating the progress of injury healing in the muscle layer. Lower panel: photomicrographs for sections form biopsies of adhesion bands developed at the site of injury stained with Masson's trichrome demonstrating the deposition of collagen fibers and development of blood vessels (magnification 100X).**

### 3.2. Experiment B: Assessment of the anti-tissue adhesion effects of MB-loaded PHB-based nanofibers and cast films in comparison to MB solution all providing 20mg/kg MB.

Based on findings of Experiment A, it could be hypothesized that the main conditions for enhancing the tissue adhesion preventing effects of the MB-loaded PHB biomaterials include the use of a relatively hydrophobic PHB matrix with relatively low porosity and small voids to reduce cell adhesion and proliferation and a relatively high MB load that bursts early into the injured tissues after surgery. Accordingly, PHB rather PHB/PEG matrices including PHB cast films were used in Experiment B. These were loaded with a larger amount of MB to provide a dose of 20mg/kg. Selection of this MB dose was based on literature data recommending MB doses up to 50 mg/kg for tissue anti-adhesion applications in rat models [268, 270, 271]. To overcome the limited loading capacity of PHB NFs, a calculated additional amount of MB was embedded by deposition of MB solution onto the matrix. Indeed, the embedding technique has been recommended as a simple method to load antimicrobial agents into a prefabricated electrospun polymer NFs matrix for tissue adhesion prevention [47].

The composition of control and test PHB-based membranes is shown in Table 8. These included PHB NFs providing a MB dose of 20mg/kg ($NF_5$, Table 8) and a PHB cast film ($CF_2$) with similar MB load. A MB solution 20 mg/kg (MB-20) and a plain PHB film ($CF_1$) were used for comparison and untreated rats (UT-B) were used as control.

#### 3.2.1. Macroscopic assessment:

Representative digital photographs of the abdominal cavity of treated rats (groups 9-12, Table 9) in comparison with untreated control rats (UT-B) at the end of the experiment are shown in Figure 38. Macroscopically, peritoneal adhesion type and extent varied with different treatments, with cast films clearly showing little adhesion of the thin filmy type. The degree of peritoneal adhesion and characteristics of adhesion bands are fully described in Table 12. Adhesion scores ± SD are shown in Figure 39. Scores were subjected to statistical analysis. Results indicated that treatment of rats with MB solution (20 mg/kg) or PHB NFs ($NF_5$) loaded with a similar total MB dose, significantly ($p<0.05$) reduced the adhesion tenacity score by 25 and 30 % respectively relative to the untreated control UT-B (90%).On the other hand, cast films resulted in an obviously greater reduction in peritoneal adhesions as indicated by the respective adhesion scores. Treatment of rats with either plain ($CF_1$) or MB-loaded ($CF_2$) PHB films significantly ($p<0.001$) reduced the extent and type scores (72 % reduction in both groups) and tenacity scores (77% reduction in both groups) in relation to the untreated positive control (85% for extent and type and 90% for tenacity). The extent, type and tenacity scores for cast films were also significantly ($p<0.001$, 0.01, respectively) lower than those of both MB solution and MB-loaded NFs. Despite similar polymer composition, striking outcomes achieved with PHB cast films can be attributed to the non-structured architecture, smoother and much less porous surface of cast films compared to NFs.

Plain and MB-loaded PHB cast films retrieved from the peritoneal cavity of rats, 14 days post-surgery showed a glossy surface seemingly free from attached tissue as shown in digital photographs in the upper panel of Figure 40. Examination of the films' fine structure by SEM

confirmed that the surface of both films was completely free from cellular growth (Lower panel in Figure 40). MB-loaded NFs ($NF_5$) did not show much cell growth on their surface (Figure 41).

Data obtained in this study verified those obtained in Experiment A regarding the implication of MB dose as an anti-adhesion pharmacological agent and the structural surface characteristics and porosity of the barrier membrane in adhesion suppression effectiveness. As comparison of tissue anti-adhesion effects of NFs and their cast film counterparts was not undertaken in previous studies, findings of the present study contribute to the development of design of tissue adhesion preventing matrices.

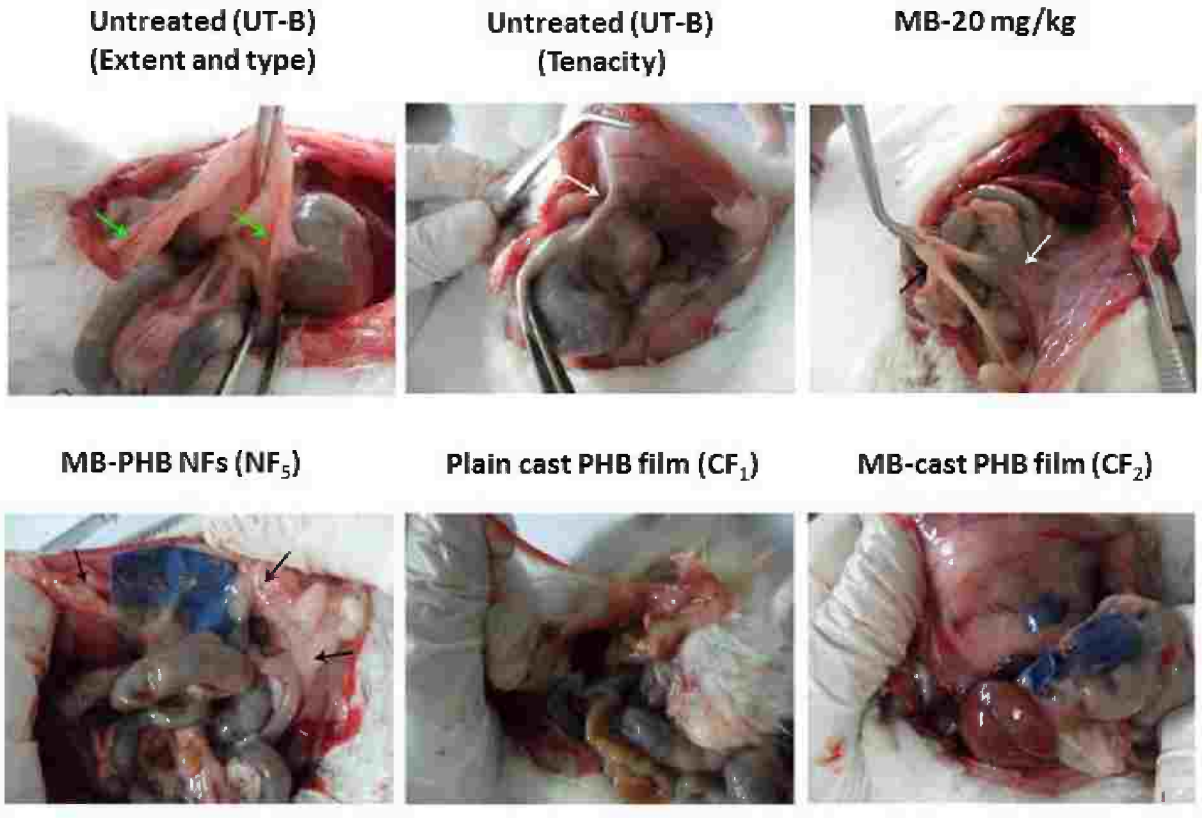


**Figure 38: Representative digital photographs for intraperitoneal adhesions in different rat groups in Experiment B.**

*Adhesion of cecum to abdominal wall (white arrows), adhesion bands (black arrows) and large blood vessels in adhesion bands (green arrows)

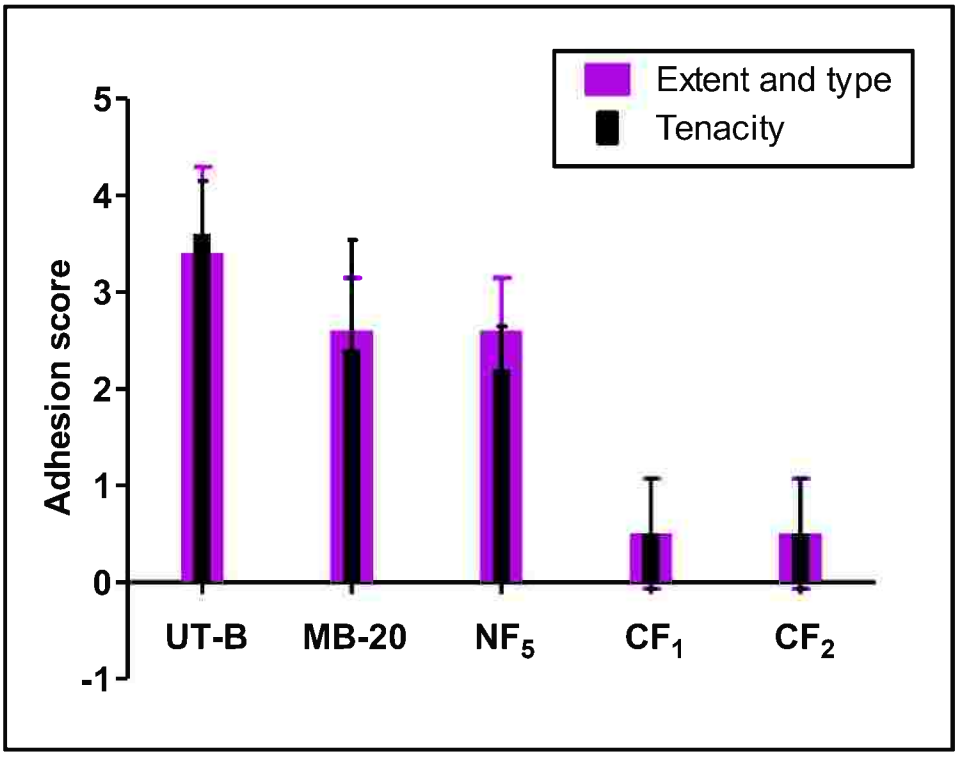


**Figure 39: Scores for adhesion extent, type and tenacity of rat groups of experiment B.**

**Table 12: General description of peritoneal adhesion of rats groups of experiment B.**

| Rat group | Code | Description of peritoneal adhesion/ Extent, type and tenacity[47, 130, 326-328] |
|---|---|---|
| 8 | UT-B | Severe opaque adhesions with larger vessels , Not dissectible without damaging organs |
| 9 | MB-20 | Moderate dense opaque avascular adhesions, Sharp / gentle dissection |
| 10 | $NF_5$ | Moderate opaque avascular adhesions, Gentle dissection |
| 11 | $CF_1$ | Filmy transparent avascular adhesions Adhesions fall apart |
| 12 | $CF_2$ | Filmy transparent avascular adhesions Adhesions fall apart |

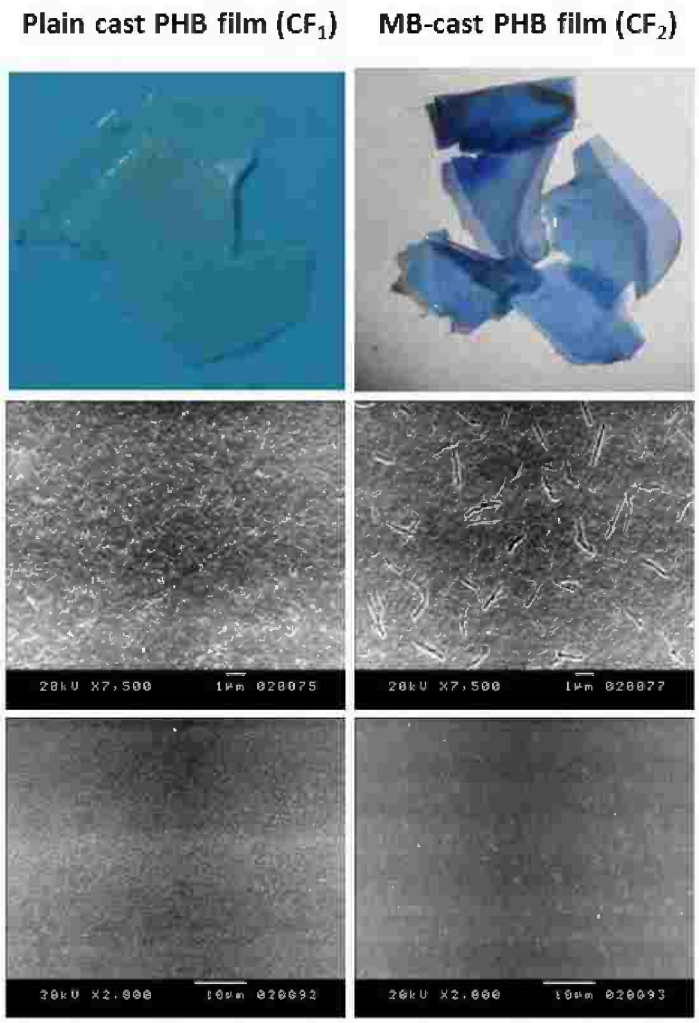


**Figure 40: Digital photographs (Upper panel) and SE micrographs of cast PHB films before implantation (Middle panel) and after implantation for 14 days in the abdominal cavities of rats (Lower panel)**

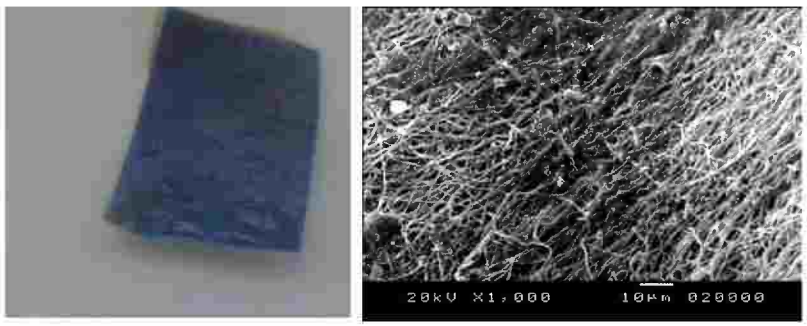


**Figure 41: Digital photograph and SE micrograph of MB-PHB NFs ($NF_5$) after implantation for 14 days in the abdominal cavities of rats.**

### 3.2.2. Histopathological examination

Histological features of biopsies from cecal tissue and adhesion bands developed at the injury site for untreated rats (UT-B) and treated rats 14 days post-surgery are shown in Figure 42.

Histopathological examination of biopsies taken from control untreated rats (UT-B) and the different treatment groups showed minimal repair of the injured serosa and muscle layer. This was associated with acute inflammation with leukocytic infiltration, edema and ulceration of the cecum muscle layer. Edema and infiltration of leukocytes extended to the submucosal layer, where dilation and congestion in the blood vessels could be observed.

While treatment with MB solution (20mg/kg) reduced the intensity of collagen fibers in the adhesion bands (Figure 42, lower panel), it did not considerably affect the healing of the cecal wall muscle layer (Figure 42, upper panel). The effect on adhesion bands was more pronounced at the 20 mg/kg relative to the 2.5 mg/kg dose level (Experiment A, Figures 42 and 37 respectively). Moreover, the effect of PHB NFs with a larger MB load and surface deposited MB in experiment B did not improve healing of the cecal wall or decrease the intensity of the collagen fibers in adhesion bands compared to PHB NFs with a lower MB load (Figures 42 and 37 respectively).

Interestingly, using a cast film barrier with the same composition as the PHB NFs ($NF_5$) but different internal structure lacking porosity and pore interconnectivity resulted in a significant enhancement of the healing of the cecal wall with minor focal edema and infiltration of leukocytes in the muscle layers (Figure 42). The intensity of collagen fibers in the adhesion bands was markedly decreased compared to groups treated with NFs membrane. Histological changes were more pronounced with the MB-loaded cast film ($CF_2$). Adhesion bands in rats treated with the plain cast film ($CF_1$) did not show evident blood capillaries and consisted of loosely arranged collagen fibers. Loading the film with MB to provide a total dose of 20 mg/kg further significantly decreased the intensity of collagen fibers deposited in the filmy adhesion bands (Figure 42).

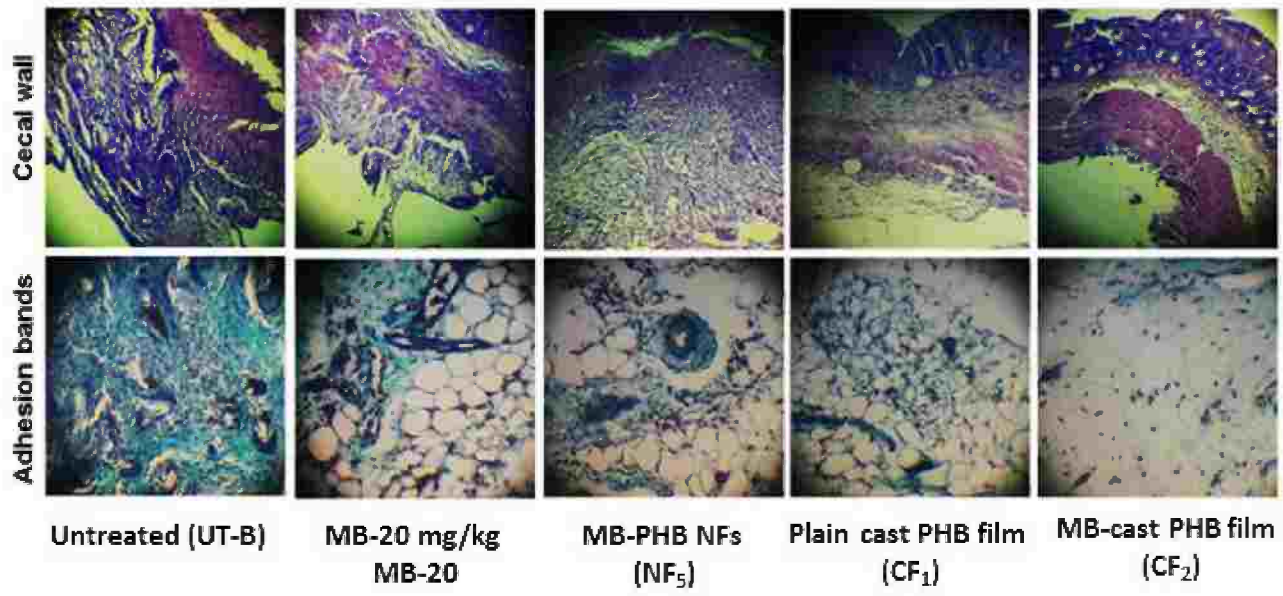


**Figure 42: Upper panel: Photomicrographs for sections from biopsies of the cecal wall of different treatment groups (Experiment B) stained with H & E (magnification 40X) demonstrating the progress of injury healing in the muscle layer. Lower panel: Photomicrographs for sections from biopsies of adhesion bands developed at the site of injury stained with Masson's trichrome showing deposition of collagen fibers and development of blood vessels (magnification 100X).**

### 3.2.3. White blood cells and neutrophils counts

Surgical incisions are known to induce an inflammatory reaction characterized by recruitment of peritoneal mesothelial cells, neutrophils, mast cells and macrophages [338]. Secretion of proinflammatory mediators, including cytokines, growth factors, nitric oxide, and reactive oxygen species (ROS) by macrophages contribute to adhesions which are modulated by polymorphonuclear leukocytes and neutrophils [339-341]. In the present study, the total white blood cell count decreased in the treated rat groups in comparison to the control group (UT-B) although differences did not reach statistical significance ($P > 0.05$). However, a significant decrease in neutrophils counts in animals treated with physical barriers (MB-loaded PHB NFs, plain cast film and MB-loaded cast film) was observed (Figure 43). Results for neutrophils count coupled with adhesion scores and histological characteristics indicated reduced inflammation.

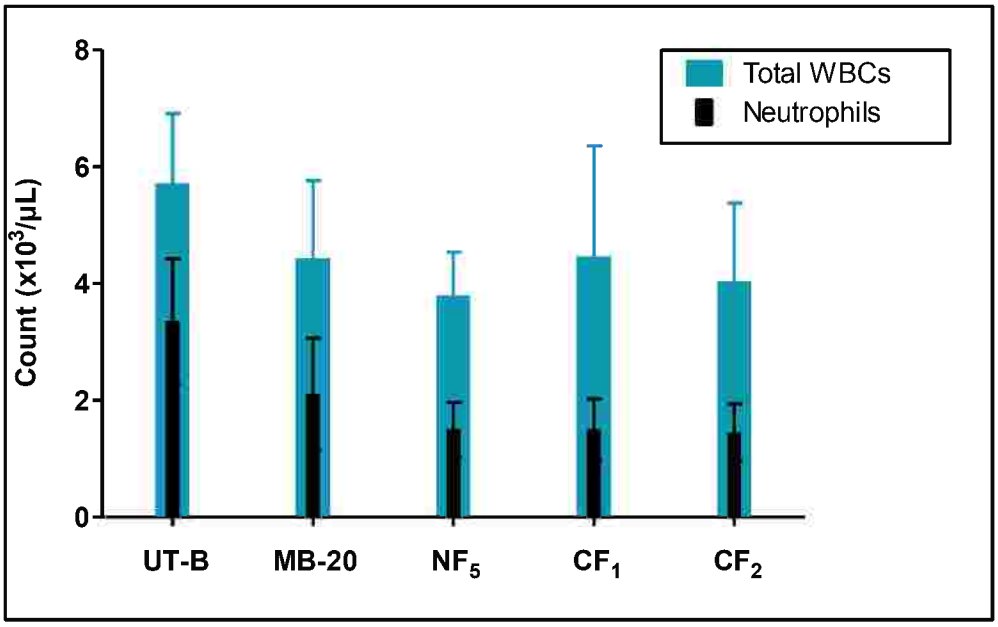


**Figure 43: Total WBCs and neutrophils in peripheral blood of different subgroups of rats of experiment B after 14 days of peritoneal adhesion induction.**

## 4. Conclusion

A new type of PHB-based biomaterials combining the tissue anti-adhesion effects of physical barriers and that of MB as a pharmacological agent with antioxidant and antimicrobial properties is presented. The membrane effectiveness was considerably affected by compositional and structural variables. The MB-loaded PHB cast film was more effective than the corresponding electrospun PHB nanofibers matrices. The combined tissue anti-adhesion effect of MB-loaded cast film was greater than the individual effects of the film matrix and MB solution. Further studies are needed to evaluate the merits of cast barrier films relative to nanofibrous matrices as tissue anti-adhesion physical barriers and determine the quality attributes of PHB cast films for the prevention of postoperative peritoneal adhesions.